BIOLOGIA (PAKISTAN)
December, 2018, 64 (II), 187-195

PKISSN 0006 – 3096 (Print)
ISSN 2313 – 206X (On-Line)

One-pot unusual synthesis and DFT studies of 3-acetyl-6-chloro-2-methyl-4-phenylquinoline and its unusual urease enhancement activity

MUHAMMAD ASLAM[1]*, ZAHRA NOREEN[2], AMINA ASGHAR[1], ABRAR HUSSAIN[2], RASHAD MEHMOOD[3], MUHAMMAD USMAN KHAN[4], KAYNAT SALEEM[5], MUHAMMAD TAHIR HUSSAIN[6]* & ASMA CHAUDHARY[7]

[1]*Department of Chemistry, Division of Science and Technology, University of Education, Township, College Road, Lahore, Pakistan*
[2]*Department of Botany, Division of Science and Technology, University of Education, College Road, Township, Lahore, Pakistan*
[3]*Department of Chemistry, University of Education, Vehari Campus, Pakistan*
[4]*Department of Applied Chemistry, Government College University, Faisalabad, Pakistan*
[5]*Department of Basic Sciences and Humanities, Khwaja Fareed University of Engineering and Information Technology, Rahim Yar Khan, Pakistan*
[6]*Department of Applied Sciences, National Textile University, Faisalabad, Pakistan*
[7]*Department of Zoology, Division of Science and Technology, University of Education, College Road, Township, Lahore, Pakistan*

ARTICLE INFORMAION

Received: 23-05-2018
Received in revised form: 20-09-2018
Accepted: 15-10-2018

***Corresponding Authors:**

Muhammad Aslam
maslamchemist@hotmail.com

Original Research Article

ABSTRACT

A surprising synthesis of 3-acetyl-6-chloro-2-methyl-4-phenylquinoline has been attained through convenient and efficient one-pot condensation of 3-chlorobenzophenone and acetylacetone. Its structure was elucidated by spectral data, X-ray diffraction studies and also investigated using density functional theory (DFT). Optimized geometry was obtained by performing DFT calculations at B3LYP level of theory and 6311+G (d,p) basis set. Frontier molecular orbital analysis has been executed at B3LYP/6-311+G(d,p) level of theory. The global reactivity parameters were explored using the energy of frontier molecular orbitals. Natural bond orbital analysis has been carried out at B3LYP/6-311+G(d,p) level of theory to discover hyper conjugative interaction and stability of the title molecule. Moreover, the product showed the reverse urease inhibition activity.

Keywords: Quinoline derivative: Schiff base: Urease inhibition activity: Density functional theory: Natural Bond Orbital: Frontier Molecular Orbital

INTRODUCTION

The diverse biological uses of Schiff bases engrossed us to synthesize some new Schiff bases (Andiappan *et al.,* 2018; Jawoor *et al.,* 2017). In this struggle, we have reported synthesis, X-ray structures and biological activities of various Schiff bases (Aslam *et al.,* 2012). In the present study, we planned to synthesize a Schiff base from 3-chlorobenzophenone and acetylacetone by the same previously used procedure but surprisingly a quinoline compound was obtained instead of the target product. Quinolines are nitrogen containing heterocyclic aromatic compounds and have diverse pharmacological activities such as antipyretic, antimalarial, analgesic, anti-inflammatory, arthritis, intracellular singling, antibiotic resistance and food preservatives etc. So herein we report the synthesis, characterization and urease activity of 3-acetyl-6-chloro-2-methyl-4-phenylquinoline. Urease activity results showed that the product enhanced the activity instead of inhibition. The urease enzyme causes the gastric ulceration, urinary stone formation, pyelonephritis, and other dysfunctions (Moncrief *et al.,* 1995). Furthermore, the synthesized compound was subjected to density functional theory (DFT) calculations to explore more about molecular geometry, electronic properties such as frontier molecular orbitals (FMOs) and natural bond orbital (NBO) analysis.

Author's Contribution: M.A., Did experimental work and wrote manuscript; **A.A.,** Designed the study, experimental design and laboratory experiments; **Z.N., A.H. & A.C.,** Did biological screening; **R.M. & M.T.H.,** Analyzed data; **M.U.K. & K.S.,** Did DFT Studies

MATERIALS AND METHODS

All the chemicals and solvents were purchased from E. Merck. TLC was performed on pre-coated silica gel G-25-UV_{254} plates (E. Merck), and detection was carried out at 254 and 366 nm. The IR spectrum was recorded on Thermo Nicolet Avatar 320 FTIR spectrometer using KBr pellets. Melting points was recorded on a Gallenkamp apparatus. Elemental analysis was performed on Perkin Elmer 2400 Series II elemental analyzer. The FAB mass spectrum was recorded on JEOL SX102/DA-6000 mass spectrometer using glycerol as matrix and ions are given in *m/z* (%). The NMR (^{1}H, ^{13}C, 2D) spectra were recorded on a Bruker AMX-400 spectrometer in DMSO-d_6. The chemical shifts (δ) are given in ppm, relative to tetramethylsilane as an internal standard, and the scalar coupling constants (*J*) are reported in Hertz. Single-crystal X-ray diffraction data was collected on Bruker Smart APEX II, CCD 4-K area detector diffractometer (Siemens 1996). Data reduction wase performed by using SAINT program. The structure was solved by direct method (Altomare *et al.,* 1993), and refined by full-matrix least squares on F2 by using the SHELXTL-PC package (Sheldrick 1997). The figures were plotted with the aid of ORTEP program (Jhnson 1976).

Procedure of the synthesis

The mixture of 2-amino-5-chlorobenzo-phenone (0.01 mole, 2.31 g) and pentane-2,4-dione (acetylacetone) (0.01 mole, 1.00 g) in ethanol (50 mL) followed by 3-4 drops of conc. H_2SO_4 was refluxed for 7 h at 70 ˚C (see synthetic scheme at Fig., 1). After cooling, the reaction mixture was concentrated to one third of its volume by rotary evaporator. The concentrated mixture was kept at room temperature for five days and white transparent crystals were obtained. The crystalline product was collected, washed with methanol and dried to afford the pure product in 87% yield. Purity of the product was checked by TLC.

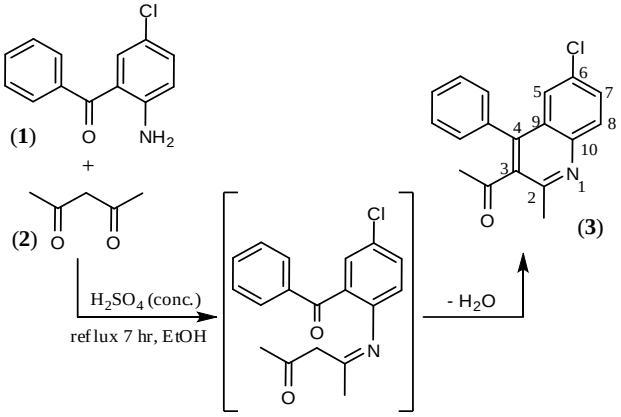

Fig. 1: Synthetic scheme of 3-Acetyl-6-chloro-2-methyl-4-phenylquinoline (**3**).

Urease inhibition assay

The urease enzyme solution was prepared by taking 0.125 units in each well in phosphate buffer ($K_2HPO_4.3H_2O$, 1 mM EDTA and 0.01M $LiCl_2$). Each well was filled with 80 μL of 0.05 M potassium phosphate buffer (pH 8.2), 10 μL of the sample (concentration range 5 - 500 μM), contents were mixed and incubated for 15 min at 30°C. 40 Microliter of substrate solution (urea, 50 mM) was poured in each well to initiate reaction. Then, 70 μL alkaline reagent (0.5 % NaOH and 0.1 % active NaOCl) and 40 μL of phenol reagent (1 % phenol and 0.005 % w/v sodium nitroprusside) were introduced to each well. The well plate, containing reaction mixture, was incubated for 50 minutes and absorbance was recorded at 630 nm. IC_{50} values were determined by monitoring the effect of increasing concentrations of the product on extent of inhibition

Computational procedure

Gaussian 09 program package (Frisch *et al.,* 2016) employing density functional theory (DFT) (Braga *et al.,* 2005) was used to perform whole computations. The initial geometry of the title molecule was retrieved from the crystal structures. Full optimization was carried out without using symmetry restrictions at B3LYP level of theory and 6-311+G(d,p) basis set. All vibrational frequencies calculated ascertain the structure is stable as no imaginary frequencies were observed. FMO and NBO analysis were performed using B3LYP level of theory with 6-311+G(d,p) basis set combination. The softwares Gauss View 5.0 (Frisch *et al.,* 2000), Avogadro (*http://avogadro.cc/wiki/Main_Page*) and Chem Craft (*http://www.chemcraftprog.com*) were used to interpret the output files results.

RESULTS AND DISCUSSION

The product, 3-acetyl-6-chloro-2-methyl-4-phenylquinoline **3**, was synthesized in good yield by the double condensation of 3-chlorobenzophenone **1** and acetylacetone **2** in the presence of few drops of conc. sulfuric acid as catalyst. The IR spectrum of the product exhibited the absorption bands at 1705 and 1606-1415 cm^{-1} for the carbonyl and the aromatic moieties, respectively. The spectrum did not show any absorption band in the range of 1630-1610 cm^{-1}, which is typical of Schiff bases (azomethine moiety) (Nicolae and Anghel 2003), indicating the product is not the expected Schiff base. The ^{1}H NMR spectrum showed the aromatic methine protons signals at δ 8.05 (1H, d, *J* = 9.2 Hz, H-8), 7.80 (1H, dd, *J* = 9.2, 2.4 Hz, H-7) and 7.39 (1H, d, *J* = 2.4 Hz, H-5). The protons of the mono-substituted benzene ring resonated at δ 7.57-

7.60 (3H, m, H-3', -4', -5') and 7.36 (2H, dd, *J* = 6.4, 2.0 Hz, H-2', -6'). The spectrum also showed two methyl singlets at δ 2.59 and 2.04, and their chemical shifts indicating their attachement with the aromatic ring and the carbonyl carbon, respectively. The absence of the methylene protons signal in the spectrum revealing that expected Schiff base product was not formed and may be methylene has been used in ring formation. The ^{13}C NMR spectrum showed a signal of the carbonyl carbon at δ 204.4 and did not show the signal of the methylene carbon. If expected Schiff base product formed then the signals of the second carbonyl and the methylene carbons must be present in the spectrum. It can be expected that one carbonyl and the methylene has been utilized in the third ring formation. In the HMBC experiment the protons at δ 7.36 (H-2', -6') showed ^{3}J correlation with the quarternary carbon at δ 142.2. It is further evidence that the carbonyl of 3-chlorobenzophenone has become the part of aromatic ring. All the HMBC and COSY correlations are shown in the Fig., 2.

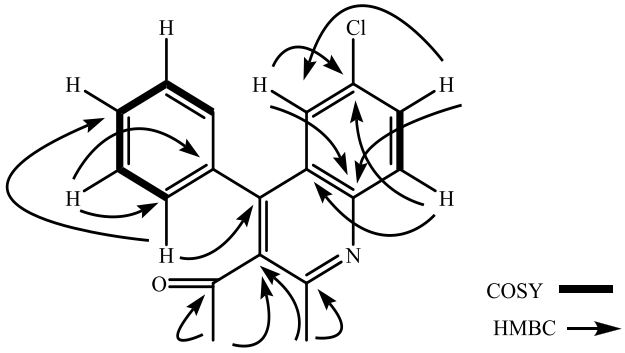

Fig. 2: All HMBC (→) and COSY (▬) correlations of the product

EIMS showed the $[M]^+$ peak at *m/z* 295 for the molecular formula $C_{18}H_{13}ClNO$. It is also comfirming that second H_2O molecule has also been removed by second condesation. Elemental analysis also fully supported the molecular formula. On the basis of all spectral data, it is evident that a double condensation has taken place during the reaction. Finally, X-ray diffraction confirmed the product structure (Fig., 3 and 4).

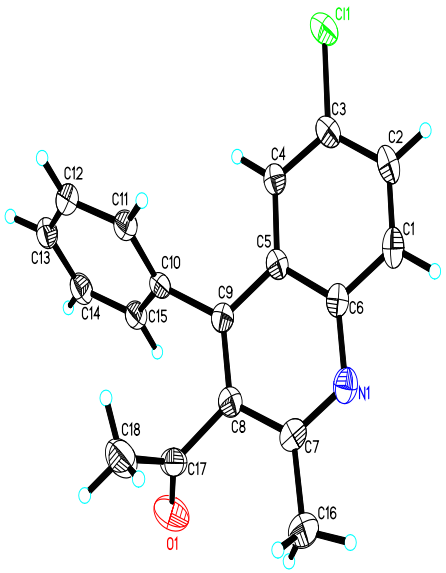

Fig. 3: The structure of the product with displacement ellipsoids drawn at 30% probability level

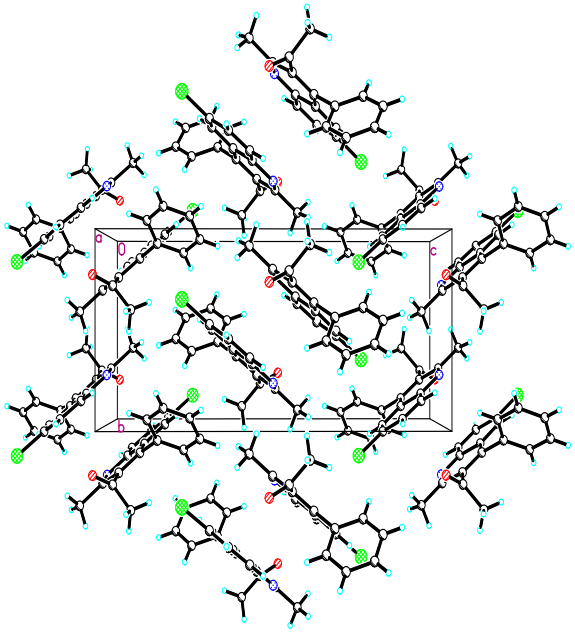

Fig. 4: The crystal packing of the product

3-Acetyl-6-chloro-2-methyl-4-phenylquinoline (3)

White crystalline solid; m.p. 154-155 ˚C; yeild 87 %; IR (KBr) v_{max} cm^{-1}; 1705 (C=O), 2923 (C-H), 1606-1415 (aromatic moiety), 700 (C-Cl); ^{1}H and ^{13}C NMR: See Table I; EI-MS (70 e/v) *m/z* (rel. int %): 295 (45, $[M]^+$), 280 (100), 252 (22), 217 (20), 176 (17); FAB-MS (+ve): 296 $[M+H]^+$ (calcd for $C_{18}H_{14}ClNO$, 296); Anal Calc. for $C_{18}H_{14}ClNO$: C 73.10; H 4.77; N 4.74. Found: C 73.15; H 5.84; N 4.70.

Table I: ^{1}H (400 MHz, DMSO-d_6) and ^{13}C (100 MHz, DMSO-d_6) NMR data of the product

C No.	C Type	δ_C	δ_H
2	C	153.9	---
3	C	135.3	---
4	C	142.4	---
5	CH	124.2	7.39 (1H, d, *J* = 2.4 Hz)
6	C	131.3	---
7	CH	130.7	7.80 (1H, dd, *J* = 9.2, 2.4 Hz)
8	CH	130.8	8.05 (1H, d, *J* = 9.2 Hz)
9	C	125.4	---
10	C	145.2	---
1'	C	133.9	---
2', 6'	CH	129.7	7.36 (2H, dd, *J* = 6.4, 2.0 Hz)
3', 5'	CH	128.9	7.57-7.60 (2H, m)
4'	CH	129.3	7.57-7.60 (1H, m)
1''	C	204.7	---
2''	CH_3	31.7	2.04 (3H, s)
1'''	CH_3	23.4	2.59 (3H, s)

X-Ray diffraction of the product

Single-crystal X-Ray diffraction analysis was carried out to establish the structure of the product. The ORTEP diagram (Fig., 3) of the product showed that the quinoline ring (C1–C9/N1) is approximately planar, with a maximum devation of 0.017 (4) Å for atom C4 and form a dihedral angle of 64.40(14)° with the mean plane of the phenyl ring (C10–C15). All bond angles and lengths were found to be in normal range (Allen *et al.,* 1987). In crystal structure no classical hydrogen bonding was found and molecules are arranged in zig zag fashion parallel to the a-axis (Fig., 4).

X-Ray crystal data of the product

$C_{18}H_{14}N_1O_1Cl_1$, Mr = 295.75, monoclinic, space group *P21/n*, *a* = 10.4798(13) Å, *b* = 8.0045(10) Å, *c* = 17.562(2) Å, *β*= 90.764(3)°, *V*= 1473.1(3) $Å^3$, *Z*=4, ρ_{calc} = 1.334 mg/m^3, *F*(000) = 616, μ(Mo Kα = 0.71073 Å, max/min transmission 0.9723 / 0.9110, crystal dimensions 0.37 x 0.29 x 0.11, 2.25◦ < θ< 25.5◦, 7930 reflections were collected, of which 2561 reflections were observed (R_{int} = 0.0411). The *R* values were: R_1 = 0.0591, wR_2 = 0.1591 for $I > 2\sigma(I)$, and R_1 = 0.0902, wR_2 = 0.1703 for all data; max/min residual electron density: 0.222 / -0.183 e $A^{\circ -3}$. Crystallographic data of the product has been deposited in the Cambridge Crystallographic Data Center. The crystallographic information can directly be obtained free of charge from CCDC data center (CCDC 883325 reference code).

Urease enhancement activity

During the urease inhibition studies of the product, it was found that it enhanced the activity instead of inhibition. To check how much it enhances, thiourea was used as standard, which showed 96 % inhibition against urease enzyme. For this, first, the product was incubated with urease for two hours and then thiourea was added and

measured the percentage inhibition, which was 62% (Table II). It shows that the product enhances the 34% activity of the enzyme or protects the enzyme from being inhibited.

Table II: Urease inhibition activities by thiourea in the absence and presence of product.

Inhibition by thiourea* in the absence of product (%)	Inhibition by thiourea in the presence of product (%)
96	62

(* Standard)

Computational Studies

Natural ond Orbital (NBO) analysis

NBO analysis is widely deployed recently to examine the bonds interaction and migration of charge densities from Lewis-type NBOs (filled or donor) to non-Lewis NBOs (vacant or acceptor) orbitals (Tahir *et al.,* 2017; Adeel *et al.,* 2017). Moreover, it is also believed that the NBO analysis is helpful for the detection of hydrogen bonding originates from hyper conjugative interactions. NBO analysis of investigated molecule was performed utilizing NBO 3.1 program which is an embedded option of Gaussian 09 package at B3LYP/6–311+G (d,p) level of theory and results are presented in Table III.

Table III: Second-order perturbation theory analysis of Fock matrix on NBO basis.

Donor(i)	Type	Acceptor (j)	Type	E(2)[a]	E(j)–E(i)[b] [a.u.]	F(i; j)[c] [a.u.]
N4-N5	π	C17-C20	π*	10.14	0.40	0.061
C9-C12	π	O3-C14	π*	18.49	0.27	0.067
C9-C12	π	C21-C25	π*	19.77	0.29	0.069
C17-C20	π	N4-N5	π*	20.09	0.23	0.064
C17-C20	π	C19-C23	π*	20.95	0.27	0.068
C19-C23	π	C17-C20	π*	17.33	0.30	0.065
C21-C25	π	C31-C33	π*	21.72	0.28	0.070
C19-C23	π	C29-C35	π*	19.85	0.30	0.069
C29-C35	π	C17-C20	π*	20.78	0.28	0.069
C31-C33	π	C9-C12	π*	22.22	0.28	0.071
C9-C14	σ	C14-C27	σ*	0.57	1.06	0.022
N5	LP(1)	C17-C20	σ*	0.62	0.97	0.022
O3	LP(2)	C14-C27	σ*	20.13	0.67	0.105

To explore the donor-acceptor interactions, second order Fock matrix was carried out using equation (Snehalatha *et al.,* 2009).

$$E^{(2)} = q_i \frac{(F_{i,j})^2}{\varepsilon_j - \varepsilon_i}$$

In above equation, $E^{(2)}$ represents the stabilization energy, q_i describes the donor-orbital occupancy, F(i,j) points out the off diagonal NBO Fock matrix elements and ε_i and ε_j represents the diagonal elements. The most credible transitions takes place in our studied systems is π(C31-C33) → π*(C9-C12) with stabilization energy value 22.22 kJ/mol. This value is the largest one among all stabilization energy values presents in investigated molecule. On the other hand, σ(C9-C14) → σ*(C14-C27) transition is found to have least energy value 0.57 kJ/mol. This transition generates weak interaction between σ (donor) and σ*(acceptor). Other transitions like π(C17-C20) → π*(C19-C23), π(C29-C35) → π*(C17-C20), π(C19-C23) → π*(C29-C35) and π(C9-C12) → π*(C21-C25) with stabilization energies 20.95, 20.78, 19.85 and 19.77 kJ/mol, respectively, represent the presence of conjugation in investigated molecule (Table III). In case of the resonance, the massive and least stabilization energy values 20.13 and 0.62 kJ/mol are observed to be for the transition LP(O3) → σ*(C14-C27) and LP(N5) → σ*(C17-C20) respectively. Above discussion confirmed the presence of extended conjugation in title molecules, hence, stabilization of the molecules due to intra-molecular hyper conjugative interactions.

Frontier Molecular Orbitals (FMOs)

HOMO and LUMO collectively form frontier molecular orbitals (FMOs). HOMO term is used to describe the highest occupied molecular orbital having higher energy, rich numbers of electron, therefore electron donating ability. Contrary, LUMO (lowest unoccupied molecular orbital) indicates the electron accepting capability due to lower energy and number deficiency of electrons. FMOs play a crucial role during molecular interactions. Furthermore, FMOs provide important perspective about the optical properties, electronic properties and reactivity of the molecule under investigation (Ebenezar *et al.,* 2013; Sun *et al.,* 2015). In this context, FMOs analysis were carried out at B3LYP (Becke, 3-parameter, Lee-Yang-Parr) level and 6311+G(d,p) basis set combination. Results of FMOs analysis are tabulated in Table IV. Four important molecular orbital pairs are examined and their pictographic display is presented in Fig., 5.

Table IV: Computed energy values for the title molecule in gas phase.

MO(s)	*E* (eV)	Δ*E* (e*V*)
HOMO	-6.82	3.75
LUMO	-3.07	
HOMO-1	-6.89	4.75
LUMO+1	-2.13	
HOMO-2	-7.22	6.00
LUMO+2	-1.21	
HOMO-3	-7.31	6.25
LUMO+3	-1.06	

E= energy, Δ*E* (e*V*) = E_{LUMO}-E_{HOMO}

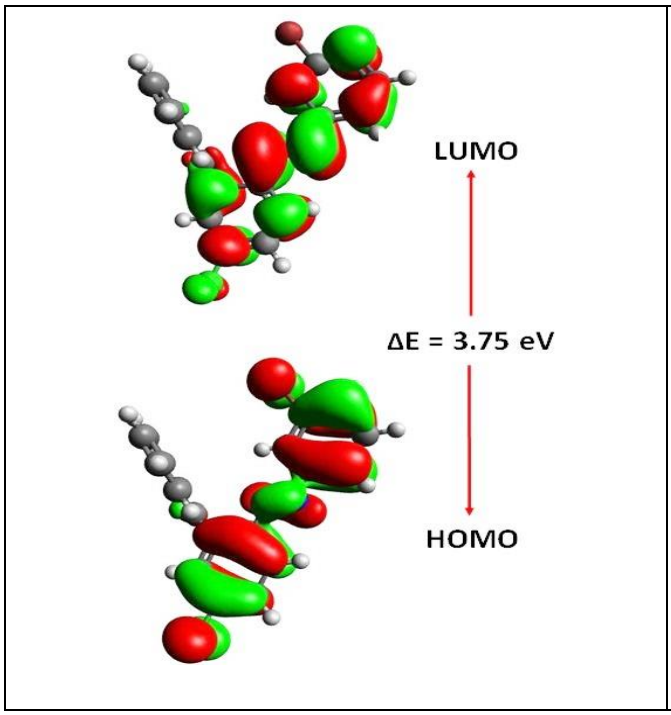

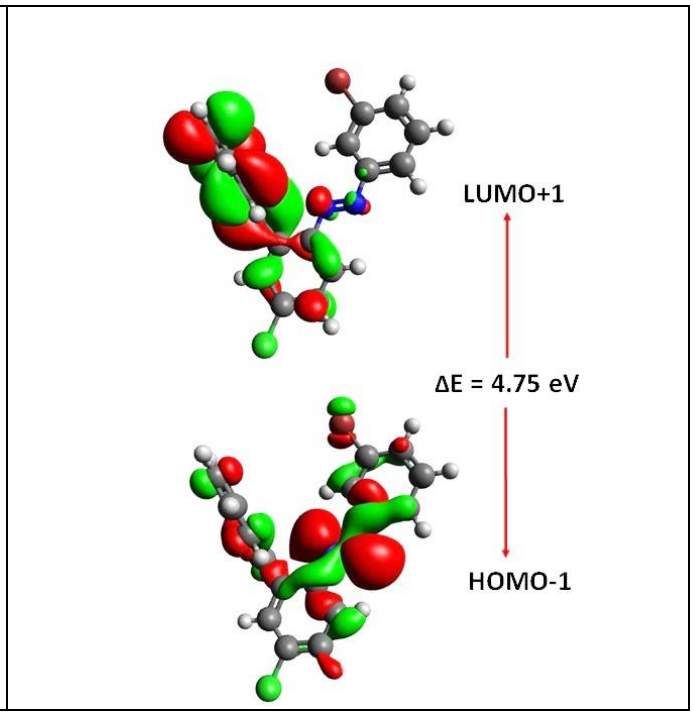

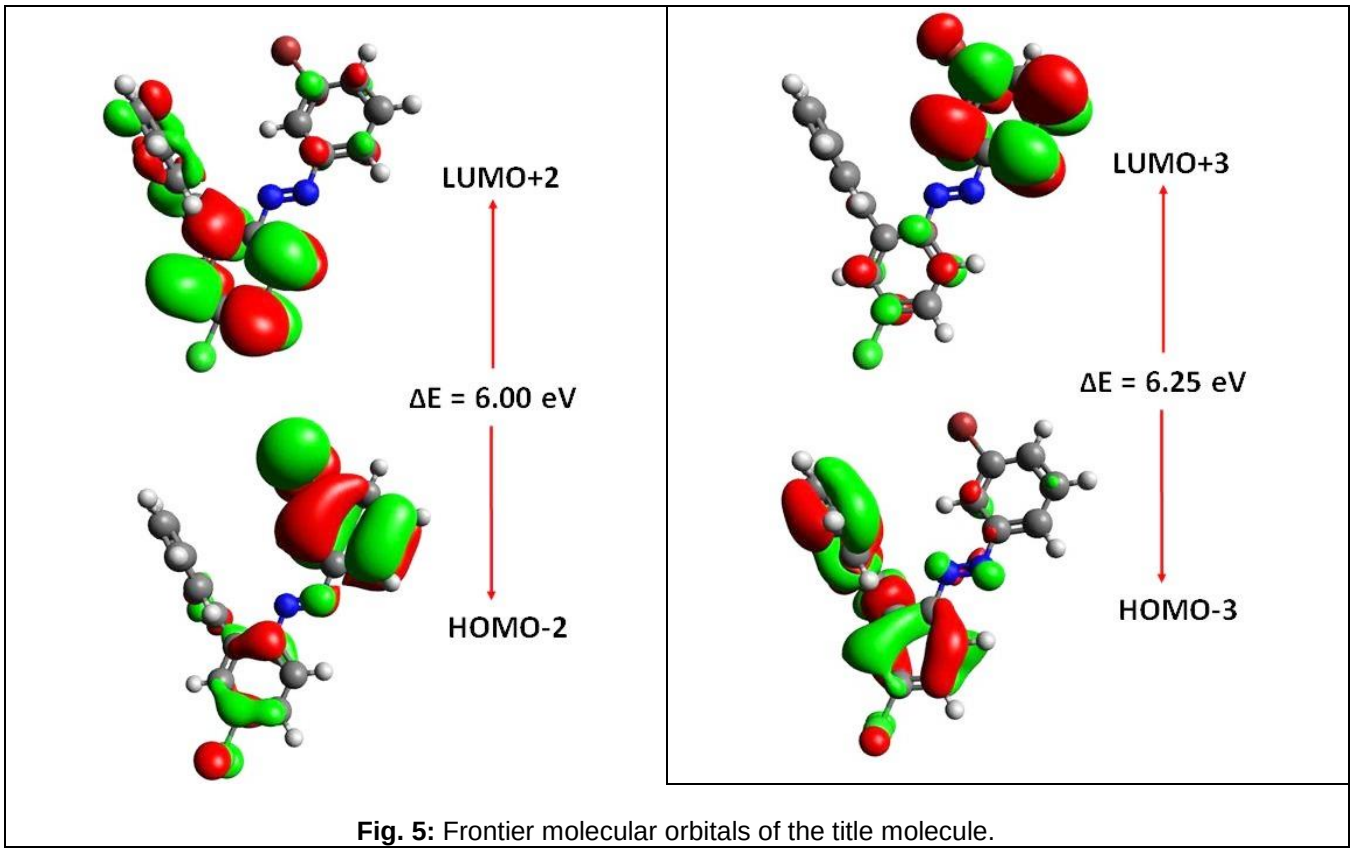

Fig. 5: Frontier molecular orbitals of the title molecule.

HOMO, LUMO are found to have energy values -6.82 and -3.07 eV respectively with an energy gap (E_{HOMO}–E_{LUMO}) value of 3.75 eV. Similarly, the calculated energy values of HOMO-1, LUMO+1 and E_{HOMO-1}–E_{LUMO+1} is found to be -6.89, -2.13 eV and 4.75 eV respectively. The energy value of HOMO-2, LUMO+2 and E_{HOMO-2} –E_{LUMO+2} is observed to be -7.22, -1.21eV and 6.00 eV, respectively. In case of HOMO-3, LUMO+3 and E_{HOMO-3}–$E_{LUMO+3,}$ the calculated energy has been found around -7.31, -1.06 eV and 6.25 eV respectively (see Table IV and Fig., 5). The energies of HOMO, LUMO and their gap play a significant function in the prediction of global reactivity descriptors (Parthasarathi *et al.,* 2004; Parthasarathi *et al.,* 2004; Mahmood *et al.,* 2015). Global reactivity descriptors, such as electrophilicity index (ω), electron affinity (EA), electronegativity (X), ionization potential (IP), global softness (S), global hardness (η) and chemical potential (μ), are calculated using following equations and results are expressed in Table V.

$$IP = -E_{HOMO}$$

$$EA = -E_{LUMO}$$

$$X = \frac{[IP + EA]}{2} = -\frac{[E_{LUMO} + E_{HOMO}]}{2}$$

$$\eta = \frac{[IP - EA]}{2} = -\frac{[E_{LUMO} - E_{HOMO}]}{2}$$

$$\mu = \frac{E_{HOMO} + E_{LUMO}}{2}$$

$$\sigma = \frac{1}{2\eta}$$

$$\omega = \frac{\mu^2}{2\eta}$$

From Table V, it is evident that the ionization potential value of title molecule is doubled than the electron affinity value which describes the better donating capability of the title molecule. Electron affinity value is found positive which depict that the investigated molecule might participate in charge transfer reactions. Electronegativity value of the title molecule is observed to be 4.952. The

electrophilicity index of the compound is found to be 6.539. Global hardness value (1.875) of title molecule is found 7 times greater than their softness value (0.266). These findings suggest that the title molecule is a hard molecule with better donating capabilities.

Table V: Ionization potential (*IP*), electron affinity (*EA*), electro negativity (*X*) chemical potential (*ì*) global hardness (*ç*) global softness (*S*) and global electrophilicity (*ù*).

	A	B	C	D
I (e*V*)	6.827	6.89	7.22	7.319
A(e*V*)	3.077	2.134	1.218	1.066
X (e*V*)	4.952	4.512	4.219	4.192
μ (e*V*)	-4.952	-4.512	-4.219	-4.192
η (e*V*)	1.875	2.378	3.001	3.126
S (e*V*)	0.266	0.210	0.166	0.159
ω (e*V*)	6.539	4.280	2.965	2.810

A= HOMO & LUMO; B= HOMO-1 & LUMO+1; C= HOMO-2 & LUMO+2; D= HOMO-3 & LUMO+3

CONCLUSION

The product was obtained by the condensation of 3-chlorobenzophenone with acetylacetone with 87% yield. Its structure was elucidated by spectroscopic data. It showed reverse urease inhibition activity i.e., it enhanced the activity instead of inhibiting. NBO analysis showed that the interaction and migration of charge densities from filled to vacant orbitals in title molecule occurred and confirmed the presence of extended conjugation that leads to stabilization of the molecule. Also the findings of FMOs suggest that the title molecule is a hard molecule with better donating capabilities.

ACKNOWLEDGMENT

Dr. Muhammad Aslam expresses his compliments to HEC Islamabad, Pakistan for providing financial support (No. 21-193/SRGP/ R&D/HEC/2014) and Department of Chemistry, University of Education, Township, Lahore for providing research facilities and also to Dr. Zahra Noreen, Dr. Abrar Hussain and Dr. Asma Chaudhary for providing facilities for biological activities.

REFERENCES

Adeel, M., Braga, A. A., Tahir, M. N., Haq, F., Khalid, M. & Halim, M. A., 2017. Synthesis, X-ray crystallographic, spectroscopic and computational studies of aminothiazole derivatives. *J. Mol. Struct*., 1131: 136-148.

Allen, F. H., Kennard, O., Watson, D. G., Brammer, L., Orpen, A. G. & Taylor, R., 1987. Tables of bond lengths determined by X-ray and neutron diffraction. Part 1. Bond lengths in organic compounds. *J. Chem. Soc. Perkin Trans.,* 2: S1-S19.

Altomare, A., Cascarano, G., Giacovazzo C. & Guagliardi, A., 1993. Completion and refinement of crystal structures with SIR92. *J. Appl. Cryst.,* 26(3): 343-350.

Andiappan, K., Sanmugam, A., Deivanayagam, E., Karuppasamy, K., Kim, H. S. & Vikraman, D., 2018. In vitro cytotoxicity activity of novel Schiff base ligand–lanthanide complexes. *Sci. Rep.*, DOI: 10.1038/s 41598-018-21366-1.

Aslam, M., Anis, I., Afza, N., Ali, B. & Shah, M. R., 2012. Synthesis, characterization and biological activities of a bidentate Schiff base ligand: *N,N′*-Bis (1-phenyl ethylidene) ethane-1,2-diamine and its transition metals (II) complexes. *J. Chem. Soc. Pak.,* 34(2): 391-395.

Braga, A. A. C., Ujaque G. & Maseras, F., 2005. A DFT study of the full catalytic cycle of the Suzuki−Miyaura cross−coupling on a model system. *Organometallics,* 25(15): 3647-3658.

Ebenezar, J. D., Ramalingam, S., Raja, C. R. & Helan, V., 2013. Precise spectroscopic [IR, Raman and NMR] investigation and gaussian hybrid computational analysis (UV-visible, NIR, MEP Maps and Kubo Gap) on L-valine. *J. Theor. Comput. Sci.,* 1: 106. DOI: 10.4172/jtco.1000106,

Frisch, A., Nielsen, A. & Holder, A., 2000. Gaussian Inc., Pittsburgh, PA.

Frisch, M. J., Trucks, G. W., Schlegel, H. B., Scuseria, G. E., Robb, M. A., Cheeseman, J. R., Scalmani, G., Barone, V., Petersson, G. A., Nakatsuji, H., Li, X., Caricato, M., Marenich, A. V., Bloino, J., Janesko, B. G., Gomperts, R., Mennucci, B., Hratchian, H. P., Ortiz, J. V., Izmaylov, A. F., Sonnenberg, J. L., Williams-Young, D., Ding, F., Lipparini, F., Egidi, F., Goings, J., Peng, B., Petrone, A., Henderson, T., Ranasinghe, D., Zakrzewski, V. G., Gao, J., Rega, N., Zheng, G., Liang, W., Hada, M., Ehara, M., Toyota, K., Fukuda, R., Hasegawa, J., Ishida, M., Nakajima, T., Honda, Y., Kitao, O., Nakai, H., Vreven, T., Throssell, K., Montgomery, J. A. Jr., Peralta, J. E., Ogliaro, F., Bearpark, M. J., Heyd, J. J., Brothers, E. N., Kudin, K. N., Staroverov, V. N., Keith, T. A., Kobayashi, R., Normand, J., Raghavachari, K., Rendell, A. P., Burant, J. C., Iyengar, S. S., Tomasi, J., Cossi, M., Millam, J. M., Klene, M., Adamo, C., Cammi, R., Ochterski, J. W., Martin, R. L., Morokuma, K., Farkas, O., Foresman, J. B. & Fox, D. J., 2016. *Gaussian, Inc., Wallingford CT.*

Jawoor, S. S., Patil, S. A. & Toragalmath, S. S., 2017. Synthesis and characterization of heteroleptic Schiff base transition metal complexes: A study of anticancer, antimicrobial, DNA cleavage and anti-TB activity. *J. Coord. Chem.,* DOI: 10.1080/00958972.2017.1421951

Jhnson, C. K., 1976. 'ORTEPII' Report ORNL-5138. Oak Ridge National Laboratory, TN, USA.

Mahmood, A., Khan, I. U., Longo, R. L., Irfan, A. & Shahzad, S. A., 2015. Synthesis and structure of 1-benzyl-5-amino-1*H*-tetrazole in the solid state and in solution: Combining X-ray diffraction, 1H NMR, FT-IR, and UV-Vis spectra and DFT calculations. *Comptes Rendus Chimie*, 18(N°4): 422-429.

Moncrief, M. B. C., Hausinger, R. P., Hom, L. G., Jabri E. & Karplus, P. A., 1995. Urease activity in the crystalline state. *Protein Sci.,* 4(10): 2234-2236.

Nicolae A. & Anghel, A., 2003. Synthesis of Schiff bases derived from 5-formyl ethylvanillin. *Analele Universităţii din Bucureşti – Chimie, Anul XII (serie nouă)*, I-II: 129-136.

Parthasarathi, R., Padmanabhan, J., Subramanian, V., Maiti, B. & Chattaraj, P. K., 2004. Toxicity analysis of 33'44'5-pentachloro-biphenyl through chemical reactivity and selectivity profiles. *Curr. Sci.,* 86(4): 535-542.

Parthasarathi, R., Padmanabhan, J., Elango, M., Subramanian, V. & Chattaraj, P. K., 2004. Intermolecular reactivity through the generalized philicity concept. *Chem. Phys. Lett*., 394(4): 225-230

Sheldrick, G. M., 1997. SHELXTL-PC (Version 5.1). In: Siemens Analytical Instruments Inc. WI, USA: Madison.

Siemens, 1996. SMART and SAINT. Siemens Analytical X-ray Instruments Inc. WI, USA: Madison.

Snehalatha, M., Ravikumar, C., Joe, I. H., Sekar N. & Jayakumar, V. 2009. Spectroscopic analysis and DFT calculations of a food additive Carmoisine. *Spectrochim. Acta. A, Mol. Biomol. Spectrosc.,* 72(3): 654-662.

Sun, L. L., Zhang, T., Wang, J., Li, H., Yan, L. K. & Su, Z. M., 2015. Exploring the influence of electron donating/withdrawing groups on hexamolybdate-based derivatives for efficient p-type dye-sensitized solar cells (DSSCs). *RSC Advances,* 5: 39821-39827.

Tahir, M. N., Khalid, M., Islam, A., Mashhadi, S. M. A. & Braga, A. A. C., 2017. Facile synthesis, single crystal analysis, and computational studies of sulfanilamide derivatives. *J. Mol. Struct.,* 1127: 766-776.